



# Impacts of reductions in anthropogenic aerosols and

# 2 greenhouse gases toward carbon neutrality on dust pollution

3 4 Shicheng Yan<sup>1,2</sup>, Yang Yang<sup>1,2\*</sup>, Lili Ren<sup>3</sup>, Hailong Wang<sup>4</sup>, Pinya Wang<sup>2</sup>, Lei Chen<sup>2</sup>, 5 Jianbin Jin<sup>1,2</sup>, Hong Liao<sup>1,2</sup> 6 7 8 9 <sup>1</sup>State Key Laboratory of Climate System Prediction and Risk Management/Jiangsu Key Laboratory of Atmospheric Environment Monitoring and Pollution 10 Control/Jiangsu Collaborative Innovation Center of Atmospheric Environment and 11 Equipment Technology/Joint International Research Laboratory of Climate and 12 Environment Change, Nanjing University of Information Science and Technology, 13 14 Nanjing, Jiangsu, China 15 <sup>2</sup>School of Environmental Science and Engineering, Nanjing University of Information Science and Technology, Nanjing, Jiangsu, China 16 <sup>3</sup>School of Environment and Ecology, Jiangsu Open University, Nanjing, Jiangsu, 17 18 China <sup>4</sup>Atmospheric, Climate, and Earth Sciences Division, Pacific Northwest National 19 20 Laboratory, Richland, Washington, USA 21 22 23 24 \*Correspondence to yang.yang@nuist.edu.cn





#### Abstract

25

26

27

28

29

30 31

32

3334

35 36

3738

39

40

41 42

To mitigate future global warming, many countries have implemented rigorous climate policies for carbon neutrality. Given some shared emission sources with greenhouse gases (GHGs), aerosol particles and their precursor emissions are expected to be reduced as the consequences of global efforts in climate mitigation and environmental improvement, potentially inducing complex climate feedbacks. Here, we assess the large-scale impacts of reductions in anthropogenic GHGs and aerosol under a carbon neutral scenario in 2060 on dust emissions and concentrations over the low- to mid-latitudes in the Northern Hemisphere using the fully coupled Community Earth System Model. Our findings demonstrate a decline in atmospheric dust loading toward carbon neutrality (SSP1-1.9) relative to the high fossil fuel scenario (SSP5-8.5). Mechanistic analysis reveals counteracting modulation mechanisms: (i) Reductions in aerosols amplify surface downwelling shortwave radiation, convection and wind speed, thereby promoting dust emissions; (ii) GHGs reductions diminish the land-ocean thermal contrast and wind speed, suppressing dust emissions. The latter drives the future dust responses. These results highlight that carbon neutral strategies not only achieve climate mitigation goals and air quality improvements, but also generate synergistic benefits through dust pollution suppression.

46

47

48 49

50

51

52 53

54 55

56 57

58

59

60

61

62

63

64

65

66

67 68

69 70

71

72

73

74

75 76





#### 1. Introduction

Dust aerosols are a crucial component of the Earth-atmosphere system, exerting multifaceted influences on environment and climate (Chen et al., 2024; Hu et al., 2023). They play a significant role in modulating the Earth's radiation budget via aerosol-cloud and aerosol-radiation interactions. Dust aerosols absorb longwave radiation and scatter shortwave radiation, thereby influencing atmospheric radiative balance and surface energy fluxes (Kok et al., 2017, 2023; Liu et al., 2021). Additionally, dust aerosols act as cloud condensation nuclei, modifying cloud microphysical properties and subsequently affecting cloud development and precipitation patterns (Min et al., 2009; Yuan et al., 2021; Zhang et al., 2021). In addition, mineral dust undergoes long-range atmospheric transport, affecting biogeochemical processes in marine ecosystems through iron deposition (Jickells et al., 2005), which stimulates phytoplankton biomass production and amplifies the biological carbon fixation efficiency (Pabortsava et al., 2017). Furthermore, dust have been demonstrated to reduce visibility, degrade air quality and have important impacts on public health, particularly in arid and semiarid regions (Fussell et al., 2021; Goudie et al., 2014; Li et al., 2024; Roy et al., 2023). These health risks are extended beyond proximal desert margins to distal urban centers by intercontinental transport mechanisms (Griffin et al., 2007; Meng et al., 2023). The global primary sources of dust emissions are located in the arid zones of the

Ine global primary sources of dust emissions are located in the arid zones of the low- to mid-latitudes in the Northern Hemisphere, with core areas concentrated in the Sahara Desert of North Africa, the Central Asia Desert, Arabian Desert, Taklamakan Desert, and Gobi Desert of East Asia, which is often called the dust belt (Prospero et al., 2002; Shao et al., 2011). Specifically, the North African desert, as the world's largest dust source, injects approximately 1.0-1.5 billion tons of dust aerosols annually into the atmosphere, accounting for 50%-65% of the global total dust emissions (Tanaka et al., 2006; Ginoux et al., 2004). Meanwhile, Asian dust sources contribute 30%-40% of the global dust flux and are identified as the second-largest emission center (Kok et al., 2021).

Dust emission is influenced by climate change, determined by a combination of natural and anthropogenic factors, including greenhouse gases (GHGs) concentrations, aerosol loading, and land use, with anthropogenic contributions exhibiting increasing influence in the post-industrial era (Gui et al., 2022; Tegen et al., 2004). Jin et al. (2017) demonstrated that the diminished Indian Ocean warming since 2002, related to the

79

80

81

82

83 84

85

86

87 88

89

90

91 92

93 94

95

96

97 98

99

100

101102

103

104105

106

107

108109

110





global warming hiatus (England et al., 2014), drove an intensification of Indian monsoon precipitation. Then the enhanced soil moisture levels, promoting vegetation expansion in northwestern India, further suppressed dust emissions (Jin et al., 2018). Additionally, variations in GHGs concentrations further regulate dust transport through large-scale atmospheric teleconnections. Elevated GHGs levels amplified the North Atlantic Oscillation (NAO) (Kuzmina et al., 2005), which changed atmospheric circulation patterns and enhanced dust advection to South Asia (Banerjee et al., 2021). The strengthened West African monsoon under warming conditions was found to amplify dust emissions (Wubben et al., 2024). In the arid and semi-arid regions of North and Central Asia, global warming-induced surface warming enhanced atmospheric instability, thereby intensifying vertical convective motions and significantly increasing dust emission fluxes (Zhou et al., 2023). Anthropogenic aerosols are recognized as an important forcing factor in global and regional climate systems (Ramanathan et al., 2001; Myhre et al., 2017). Observational analyses demonstrated that anthropogenic sulfate aerosols over the Asian monsoon region suppressed dust emissions in East Asia by altering atmospheric dynamics (Xie et al., 2025). Specifically, sulfate-induced shifts in the Asian westerly jet enhanced precipitation and reduced surface wind speeds across arid and semi-arid source regions, thereby limiting dust mobilization. Model simulations illustrated that the combined reduction of carbonaceous aerosols (black carbon and organic carbon) and increased sulfate emissions in South Asia synergistically caused atmospheric cooling over continental regions, which attenuated the zonal thermal gradient, resulting in a weakening of the Indian summer monsoon circulation (Das et al., 2020). Concurrently, this altered atmospheric circulation suppressed dust emissions from the Arabian Peninsula and inhibited dust transport across the Arabian Sea. Observational and reanalysis data from the COVID-19 pandemic period revealed that anthropogenic aerosol emission reductions over the Indian subcontinent amplified the Indian summer monsoon intensity and triggered anomalous convective activity over the tropical Indian Ocean, which increased surface wind speeds and enhanced dust lifting over the Arabian Peninsula (Francis et al., 2022). Modeling studies have demonstrated that reductions in anthropogenic aerosol emissions along the West African coast led to a decrease in aerosol loading, triggering a northward shift of the monsoonal precipitation belt. This meridional displacement subsequently enhanced surface wind speeds over the Saharan arid zone, thereby increasing mineral dust emission fluxes through intensified wind erosion processes

113114

115

116

117118

119

120121

122

123

124

125

126127

128

129

130

131132

133

134135

136137

138

139

140141

142143

144





(Menut et al., 2019).

Several studies have investigated the impact of future climate change on dust aerosols. Using the Coupled Model Intercomparison Project Phase 5 (CMIP5) multimodel simulations, Singh et al. (2017) demonstrated a 30% increase in regional dust loading over the South Asian monsoon region by the end of the 21st century (2076-2100) relative to 1976-2000 under the RCP8.5 scenario. Zhao et al. (2023) analyzed the multi-model results under four Shared Socioeconomic Pathways (SSPs) from the Coupled Model Intercomparison Project Phase 6 (CMIP6) and found that global dust loading was expected to increase by 2.0-12.5% by the end of the 21st century in most future scenarios, except for SSP3-7.0, which shows a slight decline. Liu et al. (2024) estimated a substantial increase in dust mass loading over North Africa during 2081-2100 under SSP1-2.6, SSP2-4.5, SSP3-7.0, and SSP5-8.5 scenarios from bias-corrected CMIP6 models. Woodward et al. (2005) demonstrated through HadCM3-coupled model experiments that the annual mean global dust burden would rise by 225%, from the 2000 baseline  $(4 \times 10^4 \text{ mg m}^{-2})$  to  $1.3 \times 10^5 \text{ mg m}^{-2}$  by 2100, under a medium-emission scenario, attributed to desertification and climate change. Gomez et al. (2023) projected that rising CO<sub>2</sub> concentrations would elevate global mean PM<sub>2.5</sub> levels, partly driven by intensified dust aerosol emissions attributable to a strengthened West African monsoon. Akinsanola et al. (2025) demonstrated that African easterly wave activity was projected to undergo a robust intensification across the Sahel region under both SSP2-4.5 and SSP5-8.5 scenarios by the end of the 21st century, with profound implications for Saharan dust emission and transport. However, relatively little attention has been paid to quantifying the contributions of anthropogenic aerosols and GHGs changes to the changing dust concentrations in the future, especially in the carbon-neutral scenario. Many countries have committed to achieve carbon neutrality by the middle of the 21st century to limit global temperature rise to below 2°C or even 1.5°C by the end of the 21st century. The pursuit of carbon neutrality will reshape anthropogenic emissions associated with climate and environmental policies, driving changes in atmospheric composition and radiative forcing (Wang et al., 2023; Yang et al., 2023). As nations reduce GHGs and aerosol emissions to mitigate global warming, these shifts are expected to induce complex climate influences. Studies have suggested that anthropogenic aerosol reductions could enhance surface downwelling shortwave radiation, elevate near-surface temperatures, and increase wind speed (Lei et al., 2023; Ren et al., 2024). Projections indicated that by the end of the 21st century, interannual

146

147148

149

150

151152

153

154155

156

157

158

159

160161

162

163164

165166

167

168

169 170

171





precipitation variability will intensify by 3.9% and 5.3% under 1.5°C and 2.0°C warming scenarios, respectively (Chen et al., 2020). Idealized CO<sub>2</sub> symmetric increase-decrease experiments revealed that South Asian summer monsoon precipitation exhibited asymmetric responses due to lagged tropical sea surface temperature adjustments, with enhanced El Niño-Indian Ocean Dipole-like warming during CO<sub>2</sub> ramp-down reducing monsoon rainfall through suppressed Walker circulation, triggered equatorial waves, and weakened land-sea thermal contrast, ultimately exacerbating regional drought risks (Zhang et al., 2023). Consequently, the implementation of carbon neutrality policies is likely to modify the current climate state and affect various meteorological variables (Seager et al., 2019; Lee et al., 2013), which are expected to influence dust mobilization. However, the impact of climate changes toward carbon neutrality on dust aerosols remains largely unknown.

In the carbon-neutral future, reductions in GHGs and aerosols can change climate and meteorological factors, which further affect dust emissions and concentrations. However, existing studies have yet to quantify dust response to future climate change for pursuing carbon neutrality goals and the relative contributions of anthropogenic aerosols and GHGs to dust changes. In this study, we conduct Earth system model experiments to assess the impact of aerosols and GHGs reductions on meteorological variables such as precipitation, relative humidity, and wind speed, as well as their implications for dust emissions and concentrations. Given that the combined contribution of dust sources from the North Africa and Asia exceeds 80% of global dust emissions, this study strategically focuses on the dust belt regions, including the Sahara Desert, Central Asia Desert, Arabian Desert, Taklamakan Desert, and Gobi Desert. The findings of this study aim to provide valuable insights to guide the establishment of dust prevention measures and strategies in global pursuit of carbon neutrality. The paper is structured as follows. The method and data are presented in Sect. 2. The results of dust changes related to the reductions in GHGs and aerosols are shown in Sect. 3. The discussion and the conclusions are given in Sect. 4.

172173174

175

### 2. Methods

#### 2.1 Model Description

The fully coupled Community Earth System Model version 1.2.2 (CESM1) (Hurrell et al., 2013) is used to investigate the effects of meteorological changes

180 181

182

183 184

185 186

187

188 189

190

191

192 193

194

195

196

197

198 199

200

201202

203204

205206

207

208

209210





induced by anthropogenic aerosols and GHGs under carbon neutrality on dust emissions and concentrations. The atmospheric component utilizes the Community Atmosphere Model version 5 (CAM5), which simulates the major aerosol species, including sulfate, black carbon, primary organic aerosol, secondary organic aerosol, mineral dust and sea salt. These aerosols are distributed in the four lognormal size distribution modes (i.e., Aitken, accumulation, coarse, and primary carbon modes) (Liu et al., 2016). Simulations are conducted at 1.9°×2.5° horizontal resolution with 30 vertical layers. Aerosol particles within the same mode are mixed internally, whereas external mixing assumption is treated for particles between different modes. The dust emission flux is calculated using the Dust Entrainment and Deposition model developed by Zender et al. (2003), which is implemented in the Community Land Model version 4 (CLM4; Oleson et al., 2010). Dust particles are divided into four bins  $(0.1-1.0, 1.0-2.5, 2.5-5.0, and 5.0-10.0 \mu m)$  in CLM4, and subsequently redistributed to four modes of the Modal Aerosol Module scheme. The emission or mobilization process is governed by the synergistic effects of multiple controlling parameters, including wind friction speed, vegetation cover, and surface soil moisture content. Aerosol direct and indirect radiative effects are incorporated in CAM5 (Ma et al., 2022). Furthermore, optimized parameterization schemes for key aerosol processes in CAM5, such as convective transport and wet deposition, have been implemented to enhance model performance (Wang et al., 2013). The dynamic oceanic component in CESM1 uses the Parallel Ocean Program version 2 (POP2). In this study, emissions of aerosols and precursors and GHGs concentrations are obtained from the CMIP6 input data, specifically adopting the SSP1-1.9 and SSP5-8.5 (shared socioeconomic pathways).

#### 2.2 Experimental Design

To quantify the impacts of anthropogenic aerosols and GHGs on future dust toward carbon neutrality, four sets of CESM1 simulations are designed, comprising one baseline (Fut\_SSP585) and three sensitivity experiments (Fut\_CNeutral, AA\_CNeutral and GHG\_CNeutral). The baseline simulation prescribes global GHGs concentrations and anthropogenic emissions of aerosols and precursors from the CMIP6 input data, with all forcings held at 2060 levels under the SSP5-8.5 scenario. In Fut\_CNeutral experiment, GHGs concentrations, aerosols, and their precursor emissions are adopted following SSP1-1.9 emission pathway in 2060, enabling isolation of combined effects of aerosols and GHGs through comparison with the baseline. The AA CNeutral

213214

215

216217

218219

220

221222

223224

225226

227

228

229

230231

232233

234235

236237

238239

240





experiment applies anthropogenic emissions of aerosols and precursors from SSP1-1.9 while retaining GHGs concentrations under SSP5-8.5, allowing aerosol effect quantification by comparing with the baseline. Conversely, we also perform the GHG\_CNeutral simulations in which GHGs concentrations are set to the 2060 levels under SSP1-1.9, along with aerosol emissions using SSP5-8.5 input data, which allows comparison with the baseline to estimate the climate impacts of GHGs. One additional experiment, Fut\_2020, is also performed for the model evaluation, with GHGs concentrations and aerosol emissions set to the 2020 levels under SSP1-1.9. All experiments are conducted with three ensemble members of different initial conditions, achieved by applying a small initial perturbation to atmospheric temperature. Each ensemble member is run for 100 years, with the initial 40 years considered as model spin-up period, retaining the latter 60 years for analysis.

#### 2.3 Model Evaluation

Numerous studies documented the hemispheric asymmetry of global dust sources, with most emissions originated from northern hemisphere arid zones, notably North Africa, Central Asia, East Asia, and the Middle East (Shao et al., 2011; Ginoux et al., 2012; Yang et al., 2022). Consistent with prior studies that highlight peak dust activities during boreal spring and summer in these regions (Ginoux et al., 2012; Nabavi et al., 2016; Jethva et al., 2005, Choobari et al, 2014), our seasonal analysis for simulations in 2060 also reveals substantially elevated dust emissions and concentrations in warm seasons, especially spring, compared to autumn and winter (Figure 1). In this study, we mainly focus on spring dust activities. To evaluate model's dust simulation performance, dust optical depth from model results in boreal spring of 2020 is compared with CALIPSO satellite retrievals. The model reasonably reproduces the overall spatial distribution of dust optical depth in 2020 (Figure 2), but overestimates dust loading over parts of Central Asia, Eastern Africa and the Gobi Desert. Similar discrepancies have been noted in existing studies, indicating that the deviations between the model and observations are primarily attributable to the topographic source function and the dust emission scheme used in the model (Wu et al., 2020), which could potentially lead to bias in the quantitative analysis of the results.





#### 3 Results

### 3.1 Changing dust aerosol toward carbon neutrality

Figures 3a and 3b present spatial patterns of changes in emission fluxes and near-surface concentrations of dust aerosols between carbon neutrality (SSP1-1.9) and high fossil fuel (SSP5-8.5) scenarios driven by both time-varying anthropogenic aerosols and GHGs in 2060. Under the strong decline in anthropogenic emissions toward carbon neutrality, marked reductions in dust emissions and concentrations are observed across primary source regions, particularly the North African dust belt and Central Asian arid corridor, whereas increases in dust are found over East Asian dust source regions. Dust concentrations in most regions exhibit reductions, exceeding 40 μg m<sup>-3</sup> over North Africa and Central Asia, while northwestern China and the North China Plain show a weak increase in dust concentrations.

The simulated future changes in dust concentrations are the combined effects of the reduction of anthropogenic aerosols and GHGs. Here we also investigate their respective impacts on future dust changes through sensitivity experiments. Figures 3c-d illustrate the responses of emission fluxes and near-surface concentrations of dust to anthropogenic aerosol reductions in SSP1-1.9 relative to SSP5-8.5, while 3e-f demonstrate the responses to GHGs reduction alone. The future reductions in anthropogenic aerosols would lead to significant increases in dust emissions and concentrations across the dust belt. However, GHGs reduction induces decreases in dust loads mainly over North Africa and Central Asia. These contrasting patterns indicate opposite dust responses to future reductions in anthropogenic aerosols and GHGs. The following sections illustrate possible mechanisms derived from the analysis of key meteorological drivers and their association with emission reduction strategies.

#### 3.2 Dust increases due to anthropogenic aerosols reductions

Pursuing the carbon neutrality leads to substantial reductions in anthropogenic emissions of aerosols and precursors. As shown in Figure 4, CMIP6 experiments show strong decreases in anthropogenic emissions of aerosols and precursors, including black carbon, sulfur dioxide and precursor gases of secondary organic aerosols, over polluted eastern China, South Asia, and parts of Europe and North Africa in 2060 under SSP1-1.9 scenario compared to SSP5-8.5, while primary organic matter emissions slightly increase. Along with the aerosol reduction, the surface downwelling shortwave radiation increases (Figure 5a), which further increases the land surface temperatures

276277

278

279

280281

282

283284

285

286

287

288

289290

291

292

293

294295

296

297298

299300

301

302303

304

305

306





by more than 0.6 °C over eastern China, Southeast Asia and North Afirca and 0.9 °C over South Asia (Figure 5b). Enhanced convective instability due to the warmer surface condition elevates planetary boundary layer (PBL) heights over most land regions (Figure 5c). Furthermore, diminished atmospheric heating from light-absorbing aerosols (e.g., black carbon) in the air reduces lower tropospheric stability, intensifying convective conditions and resulting in an increase in the PBL height. The associated strengthening of vertical exchange processes enhances near-surface wind speeds through downward momentum transfer (Figure 6a) (Qin et al., 2024). Related to the surface warming driven by anthropogenic aerosol reductions, relative humidity and soil water content decrease (Figures 6b and 6c). These changes in meteorological and land surface conditions explain the simulated increases in dust emissions across the dust belt due to the anthropogenic aerosol reductions toward carbon neutrality.

Previous studies have established a robust positive correlation between nearsurface wind speed and dust emission fluxes, particularly in arid dust source regions characterized by chronically low soil moisture and minimal precipitation inputs (Zender et al., 2003; Dong et al., 2006). Our analysis reveals that anthropogenic aerosol reductions in SSP1-1.9 relative to SSP5-8.5 amplify 10-m wind speed by 0.05-0.10 m s<sup>-1</sup> across core dust sources (Figures 6a), driving intensified dust emission fluxes and near-surface concentrations in North and Central Africa (Figures 3c-d). The dust-wind speed relationship is modulated by emission thresholds. In arid areas, the threshold of wind speed for dust mobilization increases with rising relative humidity (Ravi et al., 2005). This is primarily due to the enhanced adsorption layer interactions created by overlapping water films on adjacent soil particles (Ravi et al., 2005). Consequently, after the reduction of anthropogenic aerosols, reduced relative humidity by -1% to -3%(Figure 6b) lowers the critical threshold of wind speed, particularly in Central Africa and East Asia. Additionally, in the major dust source regions, precipitation changes are minimal and statistically insignificant (Figure 6d), which do not have a large influence on dust concentrations after emitting into the atmosphere.

#### 3.3 Dust decreases due to greenhouse gas reductions

Figure 7a illustrates the surface temperature distribution in 2060 under SSP5-8.5, highlighting persistent land-ocean thermal contrast with continental temperatures around dust source regions much higher than oceanic values. Due to GHGs reductions in SSP1-1.9 relative to SSP5-8.5, surface temperatures decrease by 1.8–3.0 °C over

309310

311

312313

314

315

316

317318

319

320

321322

323

324325

326

327328

329

330331

332333

334

335

336337

338339





land and 1.2–1.8 °C over adjacent oceans (Figure 7b), where the overall land-sea contrast is largely due to the higher heat capacity of water than land surface. Figures 7c and 7d respectively depict the zonal and meridional distributions of surface temperatures over the Sahara Desert of North Africa. Notably, the surface cooling due to GHGs reductions is stronger over the Sahara Desert (10°–30°N, 10°W–30°E) than that over the Mediterranean Sea (north of 30°N) and North Atlantic Ocean (west of 10°W). It diminishes the land-sea temperature gradient, thereby contributing to the decline in wind speed over North Africa (Figure 8a). Central Asia Desert also demonstrates a stronger temperature reduction than the surrounding Caspian Sea (Figure 7e) and high latitude regions, weakening the land-sea thermal gradient and thereby driving the decrease in surface wind speed throughout Central Asia (Figure 8a). As a result of the GHGs reduction implementation, the marked temperature reduction suppresses surface evaporation and alters atmospheric saturation vapor pressure, thereby increasing relative humidity across Northern Hemisphere dust source areas (Figure 8b).

Dust emission suppression in North African and Central Asian regions (Figure 3e) is primarily attributed to the weakened surface wind speeds induced by GHGs reduction (Figure 8a). The GHGs reduction elevates relative humidity (Figure 8b), which raises the critical threshold wind velocity required for dust mobilization. It further reduces dust emission fluxes and atmospheric dust concentrations, particularly in the North African and Central Asian source regions, even though the soil moisture slightly increases in some regions (Figure 8c). The precipitation does not show significant changes over the North Africa and Central Asia (Figure 8d). Over East Asia, the decreases in precipitation and soil water, likely related to the changing monsoon circulation and moisture transport due to GHGs reductions, slightly promote the dust emissions over some parts of Taklamakan Desert and Gobi Desert (Figure 3e). However, decreases in wind speed do not favor the dust transport (Figure 8a) and are conducive to the local dust deposition. It can be confirmed by the changes in dust deposition that more dust is removed from the atmosphere over the Taklamakan Desert and the downwind North China Plain (Figure 9) and the increase in dust removal surpasses the increase in dust emission (Figure 3e).

#### 4 Discussions and Conclusions

In the carbon-neutral future scenario, reductions in GHGs and aerosols for climate



341

342343

344

345

346347

348

349 350

351

352

353

354

355

356357

358

359

360361

362

363

364

365366

367

368

369370

371372

373



mitigation and environmental improvement could change meteorological conditions and further influence dust emissions and concentrations. However, critical knowledge gaps remain in dust response to future climate change for pursuing carbon neutrality goals. In this study, the impacts of anthropogenic aerosols and GHGs reductions under the global carbon neutral scenario on dust emissions and concentrations over the dust belt of low- to mid-latitudes in the Northern Hemisphere are investigated using the fully coupled CESM1 model. The distinct effects of future GHGs and aerosol emission changes on dust emissions are individually assessed. Under carbon neutral scenario (SSP1-1.9), significant reductions in dust emissions and concentrations are seen over major Asian and African dust source regions relative to the high fossil fuel scenario (SSP5-8.5) in 2060.

Anthropogenic aerosols and GHGs reduction exert opposite impacts on dust emissions. Due to aerosol reductions toward carbon neutrality, atmospheric convective is amplified, elevating surface wind speeds and intensifying dust emissions, particularly in the North African, Central Asian, South Asian, and East Asian source sectors, by year 2060. Additionally, the reduction in aerosols is expected to increase near-surface temperature by 0.3-1.2°C, decreasing relative humidity and soil water content, further intensifying dust emissions. In contrast, GHGs reduction diminishes the land-ocean thermal contrast, suppressing surface winds and associated dust emissions in North Africa and Central Asia. The marked temperature reduction also elevates relative humidity by 1-3%, suppressing dust generation, due to the GHGs reductions. Dust emissions over parts of the Taklamakan Desert and Gobi Desert are promoted, because of a decrease in precipitation and soil water. However, decreases in wind speed enhance dust deposition, leading to a decline in near-surface dust concentrations. With all these impacts considered, GHGs reductions in SSP1-1.9 compared to SSP5-8.5 in 2060 dominate dust emission decreases, surpassing contribution from future anthropogenic aerosol abatement. This study addresses the critical knowledge gaps about the dust response to future climate change for pursuing carbon neutrality, providing valuable insights to guide the establishment of dust prevention measures and strategies in global pursuit of carbon neutrality.

It should be noted that large model uncertainties exist in the projections of climate response to anthropogenic forcings, and climate simulated in CESM is relatively more sensitive to anthropogenic forcings than many other global models (Wang et al., 2023; Ren et al., 2024). Under future scenario, potential variations in tropospheric ozone

## https://doi.org/10.5194/egusphere-2025-2950 Preprint. Discussion started: 21 July 2025 © Author(s) 2025. CC BY 4.0 License.





concentrations may introduce additional complexity, as ozone can modulate key meteorological drivers as a greenhouse gas (Wang et al, 2023; Gao et al, 2022), which can also regulate dust emission processes. Furthermore, as evidenced in our model validation, the CESM dust simulations exhibit inherent limitations, primarily originating from the topographic source function and the dust emission scheme (Wu et al., 2020), which collectively contribute to systematic biases in dust emission flux estimates.





Author contributions. YY designed the research; SY performed the simulations and 381 analyzed the data. All authors including LR, HW, PW, LC, JJ and HL discussed the 382 results and wrote the paper. 383 384 385 Acknowledgments. The Pacific Northwest National Laboratory is operated for the U.S. Department of Energy by the Battelle Memorial Institute under contract DE-AC05-386 387 76RLO1830. 388 Financial support. This study was supported by the National Key Research and 389 Development Program of China (Grant 2024YFF0811400), National Natural Science 390 Foundation of China (Grant 42475032), and Jiangsu Innovation and Entrepreneurship 391 392 Team (Grant JSSCTD202346). 393 Conflict of Interest. At least one of the (co-)authors is a member of the editorial board 394 of ACP. 395 396 Code and data availability. The dust optical depth for 2020 level can be obtained from 397 398 **CALIPSO** satellite (https://search.earthdata.nasa.gov/search/granules?p=C1633034978-LARC ASDC, 399 400 last access:1 June 2025). The CESM model is publicly available at http://www.cesm.ucar.edu/models/ (last access:1 June 2025). The processed modeling 401 402 data are available at https://doi.org/10.5281/zenodo.15478736 (last access:1 June 2025).





#### References

403

429

- Akinsanola, A. A., Adebiyi, A. A., Bobde, V., Adeyeri, O. E., Tamoffo, A. T., and Danso,
   D. K.: Projected changes in African easterly wave activity due to climate change,
- 406 Commun. Earth Environ., 6, 2, https://doi.org/10.1038/s43247-024-01981-9, 2025.
- 407 Banerjee, P., Satheesh, S. K., and Krishna Moorthy, K.: Is the Atlantic Ocean driving 408 the recent variability in South Asian dust?, Atmos. Chem. Phys., 21, 17665–17685, 409 https://doi.org/10.5194/acp-21-17665-2021, 2021.
- Chen, Y., Chen, S., Bi, H., Zhou, J., and Zhang, Y.: Where is the Dust Source of 2023
  Several Severe Dust Events in China?, Bull. Amer. Meteor. Soc., 105, E2085–
  E2096, https://doi.org/10.1175/BAMS-D-23-0121.1, 2024.
- Chen, Z., Zhou, T., Zhang, W., Li, P., and Zhao, S.: Projected changes in the annual range of precipitation under stabilized 1.5°C and 2.0°C warming futures, Earth's Future, 8, e2019EF001435, https://doi.org/10.1029/2019EF001435, 2020.
- Choobari, O. A., Zawar-Reza, P., and Sturman, A.: The global distribution of mineral
   dust and its impacts on the climate system: A review, Atmos. Res., 138, 152-165,
   https://doi.org/10.1016/j.atmosres.2013.11.007, 2014.
- Das, S., Giorgi, F., Giuliani, G., Dey, S., and Coppola, E.: Near-future anthropogenic aerosol emission scenarios and their direct radiative effects on the present-day characteristics of the Indian summer monsoon, J. Geophys. Res-atmos., 125, e2019JD031414, https://doi.org/10.1029/2019JD031414, 2020.
- Dong, Z., Wang, H., Qian, G., Luo, W., and Zhang, Z.: Wind shear with a blowing-sand boundary layer, Geophys. Res. Lett., 33, L22804, https://doi.org/10.1029/2006GL026739, 2006.
- England, M. H., McGregor, S., Spence, P., Meehl, G. A., Timmermann, A., Cai, W.,
  Gupta, A. S., McPhaden, M. J., Purich, A., and Santoso, A.: Recent intensification
  of wind-driven circulation in the Pacific and the ongoing warming hiatus, Nat.

Clim. Change, 4, 222–227, https://doi.org/10.1038/nclimate2106, 2014.

- Francis, D., Fonseca, R., Nelli, N., Teixido, O., Mohamed, R., and Perry, R.: Increased
  Shamal winds and dust activity over the Arabian Peninsula during the COVID-19
  lockdown period in 2020, Aeolian Res., 55, 100786,
  https://doi.org/10.1016/j.aeolia.2022.100786, 2022.
- Fussell, J. C., and Kelly, F. J.: Mechanisms underlying the health effects of desert sand dust, Environ. Int., 157, 106790, https://doi.org/10.1016/j.envint.2021.106790, 2021.
- Gao, J., Yang, Y., Wang, H., Wang, P., Li, H., Li, M., Ren, L., Yue, X., and Liao, H.:
  Fast climate responses to emission reductions in aerosol and ozone precursors in
  China during 2013–2017, Atmos. Chem. Phys., 22, 7131–7142,
  https://doi.org/10.5194/acp-22-7131-2022, 2022.
- Ginoux, P., Prospero, J. M., Gill, T. E., Hsu, N. C., and Zhao, M.: Global-scale attribution of anthropogenic and natural dust sources and their emission rates





- based on MODIS Deep Blue aerosol products, Rev. Geophys., 50, RG3005, https://doi.org/10.1029/2012RG000388, 2012.
- Ginoux, P., Prospero, J. M., Torres, O., and Chin, M.: Long-term simulation of global
   dust distribution with the GOCART model: correlation with North Atlantic
   Oscillation, Environ. Modell. Softw., 19, 113-128, https://doi.org/10.1016/S1364-

8152(03)00114-2, 2004.

- Gomez, J., Allen, R. J., Turnock, S. T., Horowitz, L. W., Tsigaridis, K., Bauer, S. E.,
  Olivié, D., Thomson, E. S., and Ginoux, P.: The projected future degradation in air
  quality is caused by more abundant natural aerosols in a warmer world, Commun.
  Earth Environ., 4, 22, https://doi.org/10.1038/s43247-023-00688-7, 2023.
- Goudie, A. S.: Desert dust and human health disorders, Environ. Int., 63, 101-113, https://doi.org/10.1016/j.envint.2013.10.011, 2014.
- 455 Griffin, D. W.: Atmospheric Movement of Microorganisms in Clouds of Desert Dust 456 and Implications for Human Health, Clin. Microbiol. Rev., 20, 459-477, 457 https://doi.org/10.1128/cmr.00039-06, 2007.
- Gui, K., Yao, W., Che, H., An, L., Zheng, Y., Li, L., Zhao, H., Zhang, L., Zhong, J., Wang, Y., and Zhang, X.: Record-breaking dust loading during two mega dust storm events over northern China in March 2021: aerosol optical and radiative properties and meteorological drivers, Atmos. Chem. Phys., 22, 7905–7932, https://doi.org/10.5194/acp-22-7905-2022, 2022.
- Hu, Z., Ma, Y., Jin, Q., Idrissa, N. F., Huang, J., and Dong, W.: Attribution of the March
  2021 exceptional dust storm in North China, Bull. Am. Meteorol. Soc., 104, E749–
  E755, https://doi.org/10.1175/BAMS-D-22-0151.1, 2023.
- Hurrell, J. W., Holland, M. M., Gent, P. R., Ghan, S., Kay, J. E., Kushner, P. J.,
  Lamarque, J. F., Large, W. G., Lawrence, D., Lindsay, K., Lipscomb, W. H., Long,
  M. C., Mahowald, N., Marsh, D. R., Neale, R. B., Rasch, P., Vavrus, S., Vertenstein,
  M., Bader, D., Collins, W. D., Hack, J. J., Kiehl, J., and Marshall, S.: The
  Community Earth System Model: A Framework for Collaborative Research, Bull.
  Am. Meteor. Soc., 94, 1339–1360, https://doi.org/10.1175/BAMS-D-12-00121.1,
  2013.
- Jethva, H., Satheesh, S. K., and Srinivasan, J.: Seasonal variability of aerosols over the
   Indo-Gangetic basin, J. Geophys. Res., 110, D21204,
   https://doi.org/10.1029/2005JD005938, 2005.
- Jickells, T. D., An, Z. S., Andersen, K. K., Baker, A. R., Bergametti, G., Brooks, N.,
  Cao, J. J., Boyd, P. W., Duce, R. A., Hunter, K. A., Kawahata, H., Kubilay, N.,
  Laroche, J., Liss, P. S., Mahowald, N., Prospero, J. M., Ridgwell, A. J., Tegen, I.,
  and Torres, R.: Global Iron Connections Between Desert Dust, Ocean
  Biogeochemistry, and Climate, Science, 308, 67-71,

481 https://doi.org/10.1126/science.1105959, 2005.





- Jin, Q., and Wang, C.: A revival of Indian summer monsoon rainfall since 2002, Nat. Clim. Change, 7, 587–594, https://doi.org/10.1038/nclimate3348, 2017.
- Jin, Q., and Wang, C.: The greening of Northwest Indian subcontinent and reduction of dust abundance resulting from Indian summer monsoon revival, Sci. Rep., 8, 4573, https://doi.org/10.1038/s41598-018-23055-5, 2018.
- Kok, J. F., Adebiyi, A. A., Albani, S., Balkanski, Y., Checa-Garcia, R., Chin, M.,
  Colarco, P. R., Hamilton, D. S., Huang, Y., Ito, A., Klose, M., Li, L., Mahowald,
  N. M., Miller, R. L., Obiso, V., Pérez García-Pando, C., Rocha-Lima, A., and Wan,
  J. S.: Contribution of the world's main dust source regions to the global cycle of
  desert dust, Atmos. Chem. Phys., 21, 8169–8193, https://doi.org/10.5194/acp-21-8169-2021, 2021.
- Kok, J. F., Ridley, D. A., Zhou, Q., Miller, R. L., Zhao, C., Heald, C. L., Ward, D. S.,
  Albani, S., and Haustein, K.: Smaller desert dust cooling effect estimated from
  analysis of dust size and abundance, Nat. Geosci., 10, 274–278,
  https://doi.org/10.1038/ngeo2912, 2017.
- Kok, J.F., Storelvmo, T., Karydis, V.A., Adebiyi, A. A., Mahowald, N. M., Evan, A. T.,
  He, C., and Leung, D. M.: Mineral dust aerosol impacts on global climate and
  climate change, Nat. Rev. Earth Environ., 4, 71–86,
  https://doi.org/10.1038/s43017-022-00379-5, 2023.
- Kuzmina, S. I., Bengtsson, L., Johannessen, O. M., Drange, H., Bobylev, L. P., and
   Miles, M. W.: The North Atlantic Oscillation and greenhouse-gas forcing,
   Geophys. Res. Lett., 32, L04703, https://doi.org/10.1029/2004GL021064, 2005.
- Lee, S., and Feldstein, S. B.: Detecting Ozone- and Greenhouse Gas-Driven Wind Trends with Observational Data, Science, 339, 563-567, https://doi.org/10.1126/science.1225154, 2013.
- Lei, Y., Wang, Z., Wang, D., Zhang, X., Chen, H., Yue, X., Tian, C., Zhong, J., Guo, L.,
  Li, L., Zhou, H., Liu, L., and Xu, Y.: Co-benefits of carbon neutrality in enhancing
  and stabilizing solar and wind energy, Nat. Clim. Chang, 13, 693–700,
  https://doi.org/10.1038/s41558-023-01692-7, 2023.
- Li, B., Liao, H., Li, K., Wang, Y., Zhang, L., Guo, Y., Liu, L., Li, J., Jin, J., Yang, Y.,
  Gong, C., Wang, T., Shen, W., Wang, P., Dang, R., Liao, K., Zhu, Q., and Jacob,
  D. J.: Unlocking nitrogen management potential via large-scale farming for air
  quality and substantial Co-benefits, Natl. Sci. Rev., 11, nwae324,
  https://doi.org/10.1093/nsr/nwae324, 2024.
- Liu, J., Wang, X., Wu, D., Wei, H., Li, Y., and Ji, M.: Historical footprints and future projections of global dust burden from bias-corrected CMIP6 models, npj Clim. Atmos. Sci., 7, 1, https://doi.org/10.1038/s41612-023-00550-9, 2024.
- Liu, X., Chen, S., Guo, Z., Zhou, H., Chen, Y., Kang, Y., Liu, Q., Huang, G., Liu, T., Chen, C., and He, Q.: The influence of dusts on radiation and temperature over the





- eastern Asia with a regional climate model, Sci. Total Environ., 792, 148351,
- 522 https://doi.org/10.1016/j.scitotenv.2021.148351, 2021.
- 523 Liu, X., Ma, P.-L., Wang, H., Tilmes, S., Singh, B., Easter, R. C., Ghan, S. J., and Rasch,
- 524 P. J.: Description and evaluation of a new four-mode version of the Modal Aerosol
- Module (MAM4) within version 5.3 of the Community Atmosphere Model,
- 526 Geosci. Model Dev., 9, 505–522, https://doi.org/10.5194/gmd-9-505-2016, 2016.
- 527 Ma, X., Huang, G., and Cao, J.: The significant roles of anthropogenic aerosols on
- surface temperature under carbon neutrality, Sci. Bull., 67, 470-473,
- 529 https://doi.org/10.1016/j.scib.2021.10.022, 2022.
- Meng, Q., Yan, C., Li, R., Zhang, T., Zheng, M., Liu, Y., Zhang, M., Wang, G., Du, Y.,
- 531 Shang, C., and Fu, P.: Variations of PM2.5-bound elements and their associated
- effects during long-distance transport of dust storms: Insights from multi-sites
- observations, Sci. Total Environ, 889, 164062,
- https://doi.org/10.1016/j.scitotenv.2023.164062, 2023.
- 535 Menut, L., Tuccella, P., Flamant, C., Deroubaix, A., and Gaetani, M.: The role of
- aerosol-radiation-cloud interactions in linking anthropogenic pollution over
- southern west Africa and dust emission over the Sahara, Atmos. Chem. Phys., 19,
- 538 14657-14676, https://doi.org/10.5194/acp-19-14657-2019, 2019.
- Min, Q. L., Li, R., Lin, B., Joseph, E., Wang, S., Hu, Y., Morris, V., and Chang, F.:
- Evidence of mineral dust altering cloud microphysics and precipitation, Atmos.
- 541 Chem. Phys., 9, 3223–3231, https://doi.org/10.5194/acp-9-3223-2009, 2009.
- 542 Myhre, G., Forster, P. M., Samset, B. H., Hodnebrog, Ø., Sillmann, J., Aalbergsjø, S.
- 543 G., Andrews, T., Boucher, O., Faluvegi, G., Fläschner, D., Iversen, T., Kasoar, M.,
- Kharin, V., Lamarque, J. F., Olivié, D., Richardson, T., Shindell, D., Shine, K. P.,
- 545 Stjern, C. W., Takemura, T., Voulgarakis, A., and Zwiers, F.: PDRMIP: A
- 546 Precipitation Driver and Response Model Intercomparison Project, Protocol and
- 547 preliminary results, Bull. Am. Meteorol. Soc., 98(6), 1185-1198.
- 548 https://doi.org/10.1175/bams-d-16-0019.1, 2017.
- Nabavi, S. O., Haimberger, L., and Samimi, Cyrus.: Climatology of dust distribution
- over West Asia from homogenized remote sensing data, Aeolian Res., 21, 93-107,
- 551 https://doi.org/10.1016/j.aeolia.2016.04.002, 2016.
- 552 Oleson, K. W., Lawrence, D. M., Bonan, G. B., Flanner, M. G., Kluzek, E., Lawrence,
- P. J., Levis, S., Swenson, S. C., Thornton, P. E., Dai, A., and Decker, M.: Technical
- description of version 4.0 of the Community Land Model (CLM) (NCAR/TN-
- 555 478+STR), University Corporation for Atmospheric Research,
- 556 https://doi.org/10.5065/D6FB50WZ, 2010.
- 557 Pabortsava, K., Lampitt, R. S., Benson, J., Crowe, C., McLachlan, R., Moigne, F. A.,
- Moore, C. M., Pebody, C., Provost, P., Rees, A. P., Tilstone, G. H., and Woodward,
- 559 E. M. S.: Carbon sequestration in the deep Atlantic enhanced by Saharan dust, Nat.
- Geosci., 10, 189–194, https://doi.org/10.1038/ngeo2899, 2017.





- Prospero, J. M., Ginoux, P., Torres, O., Nicholson, S. E., and Gill, T. E.: Environmental
- characterization of global sources of atmospheric soil dust identified with the
- nimbus 7 total ozone mapping spectrometer (TOMS) absorbing aerosol product,
- Rev. Geophys., 40(1), 1002, https://doi.org/10.1029/2000RG000095, 2002.
- Oin, Y., Zhou, M., Hao, Y., Huang, X., Tong, D., Huang, L., Zhang, C., Cheng, J., Gu,
- W., Wang, L., He, X., Zhou, D., Chen, Q., Ding, A., and Zhu, T.: Amplified
- positive effects on air quality, health, and renewable energy under China's carbon
- neutral target, Nat. Geosci., 17, 411–418, https://doi.org/10.1038/s41561-024-
- 569 01425-1, 2024.
- 870 Ramanathan, V., Crutzen, P. J., Kiehl, J. T., and Rosenfeld, D.: Aerosols, Climate, and
- 571 the Hydrological Cycle, Science, 294, 2119-2124,
- 572 https://doi.org/10.1126/science.1064034, 2001.
- 873 Ravi, S., and D'Odorico, P.: A field-scale analysis of the dependence of wind erosion
- 574 threshold velocity on air humidity, Geophys. Res. Lett., 32, L21404,
- 575 https://doi.org/10.1029/2005GL023675, 2005.
- 876 Ren, L., Yang, Y., Wang, H., Wang, P., Yue, X., and Liao, H.: Co-benefits of mitigating
- aerosol pollution to future solar and wind energy in China toward carbon neutrality,
- 578 Geophys. Res. Lett., 51, e2024GL109296,
- 579 https://doi.org/10.1029/2024GL109296, 2024.
- Roy, D., Kim, J., Lee, M., and Park, J.: Adverse impacts of Asian dust events on human
- health and the environment—A probabilistic risk assessment study on particulate
- matter-bound metals and bacteria in Seoul, South Korea, Sci. Total Environ., 875,
- 583 162637, https://doi.org/10.1016/j.scitotenv.2023.162637, 2023.
- 584 Seager, R., Cane, M., Henderson, N., Lee, D., Abernathey, R., and Zhang, H.:
- 585 Strengthening tropical Pacific zonal sea surface temperature gradient consistent
- with rising greenhouse gases, Nat. Clim. Change, 9, 517–522.
- 587 https://doi.org/10.1038/s41558-019-0505-x, 2019.
- 588 Shao, Y., Wyrwoll, K.-H., Chappell, A., Huang, J., Lin, Z., McTainsh, G. H., Mikami,
- M., Tanaka, T. Y., Wang, X., and Yoon, S.: Dust cycle: An emerging core theme in
- 590 Earth system science, Aeolian Res., 2, 181-204,
- 591 https://doi.org/10.1016/j.aeolia.2011.02.001, 2011.
- 592 Singh, C., Ganguly, D., and Dash, S. K.: Dust load and rainfall characteristics and their
- 593 relationship over the South Asian monsoon region under various warming
- 594 scenarios, J. Geophys. Res. Atmos., 122, 7896-7921,
- 595 https://doi.org/10.1002/2017JD027451, 2017.
- 596 Tanaka, T. Y., and Chiba, M.: A numerical study of the contributions of dust source
- regions to the global dust budget, Glob. Planet. Change, 52, 88-104,
- 598 https://doi.org/10.1016/j.gloplacha.2006.02.002, 2006.





- Tegen, I., Werner, M., Harrison, S. P., and Kohfeld, K. E.: Relative importance of climate and land use in determining present and future global soil dust emission, Geophys. Res. Lett., 31, L05105, https://doi.org/10.1029/2003GL019216, 2004.
- Wang, H., Easter, R. C., Rasch, P. J., Wang, M., Liu, X., Ghan, S. J., Qian, Y., Yoon, J. H., Ma, P.-L., and Vinoj, V.: Sensitivity of remote aerosol distributions to
   representation of cloud–aerosol interactions in a global climate model, Geosci.
   Model Dev., 6, 765–782, https://doi.org/10.5194/gmd-6-765-2013, 2013.
- Wang, P., Yang, Y., Xue, D., Ren, L., Tang, J., Leung, L. R., and Liao, H.: Aerosols
   overtake greenhouse gases causing a warmer climate and more weather extremes
   toward carbon neutrality, Nat. Commun., 14, 7257,
   https://doi.org/10.1038/s41467-023-42891-2, 2023.
- Woodward, S., Roberts, D. L., and Betts, R. A.: A simulation of the effect of climate
   change-induced desertification on mineral dust aerosol, Geophys. Res. Lett., 32,
   L18810, https://doi.org/10.1029/2005GL023482, 2005.
- Wu, M., Liu, X., Yu, H., Wang, H., Shi, Y., Yang, K., Darmenov, A., Wu, C., Wang, Z.,
  Luo, T., Feng, Y., and Ke, Z.: Understanding processes that control dust spatial
  distributions with global climate models and satellite observations, Atmos. Chem.
  Phys., 20, 13835–13855, https://doi.org/10.5194/acp-20-13835-2020, 2020.
- Wubben, E., Spiering, B. R., Veenstra, T., Bos, R., Wang, Z., van Dijk, J., Raffi, I.,
  Witkowski, J., Hilgen, F. J., Peterse, F., Sangiorgi, F., and Sluijs, A.: Tropical
  warming and intensification of the West African Monsoon during the Miocene
  Climatic Optimum, Paleoceanogr. Paleoclimatol., 39, e2023PA004767,
  https://doi.org/10.1029/2023PA004767, 2024.
- Xie, X., Myhre, G., Che, H., Wu, F., Guo, J., Shi, Z., Li, X., Liu, X., and Liu, Y.:
   Anthropogenic sulfate-climate interactions suppress dust activity over East Asia,
   Commun. Earth Environ., 6, 159, https://doi.org/10.1038/s43247-025-02147-x,
   2025.
- Yang, Y., Zeng, L., Wang, H., Wang, P., and Liao, H.: Climate effects of future aerosol
   reductions for achieving carbon neutrality in China, Sci. Bull., 68, 902-905,
   https://doi.org/10.1016/j.scib.2023.03.048, 2023.
- Yang, Y., Zeng, L., Wang, H., Wang, P., and Liao, H.: Dust pollution in China affected
   by different spatial and temporal types of El Niño, Atmos. Chem. Phys., 22,
   14489–14502, https://doi.org/10.5194/acp-22-14489-2022, 2022.
- Yuan, T., Huang J., Cao J., Zhang G., and Ma X.: Indian dust-rain storm: Possible
   influences of dust ice nuclei on deep convective clouds, Sci. Total Environ., 779,
   146439, https://doi.org/10.1016/j.scitotenv.2021.146439, 2021.
- Zender, C. S., Bian, H., and Newman, D.: Mineral Dust Entrainment and Deposition
   (DEAD) model: Description and 1990s dust climatology, J. Geophys. Res., 108,
   4416, https://doi.org/10.1029/2002JD002775, D14, 2003.





638	Zhang, S., Qu, X., Huang, G., and Hu, P.: Asymmetric response of South Asian summer
639	monsoon rainfall in a carbon dioxide removal scenario, npj Clim. Atmos. Sci., 6,
640	10, https://doi.org/10.1038/s41612-023-00338-x, 2023.
641	Zhang, Y., Yu, F., Luo, G., Fan, J., and Liu, S.: Impacts of long-range-transported
642	mineral dust on summertime convective cloud and precipitation: a case study over
643	the Taiwan region, Atmos. Chem. Phys., 21, 17433-17451,
644	https://doi.org/10.5194/acp-21-17433-2021, 2021.
645	Zhao, Y., Yue, X., Cao, Y., Zhu, J., Tian, C., Zhou, H., Chen, Y., Hu, Y., Fu, W., and
646	Zhao, X.: Multi-model ensemble projection of the global dust cycle by the end of
647	21st century using the Coupled Model Intercomparison Project version 6 data,
648	Atmos. Chem. Phys., 23, 7823-7838, https://doi.org/10.5194/acp-23-7823-2023,
649	2023.
650	Zhou, Y., Wu, T., Zhou, Y., Zhang, J., Zhang, F., Su, X., Jie, W., Zhao, H., Zhang, Y.,
651	and Wang, J.: Can global warming bring more dust?, Clim. Dyn., 61, 2693-2715,
652	https://doi.org/10.1007/s00382-023-06706-w, 2023.





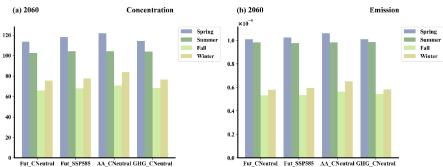


**Figure 1.** Seasonal mean (a) dust near-surface concentration (µg m $^{-3}$ ) and (b) dust emission (kg m $^{-2}$  s $^{-1}$ ) during boreal spring (March-April-May), summer (June-July-August), Autumn (September-October-November) and winter (December-January-February) of 2060 over the dust belt (0°–60°N, 25°W–130°E) simulated from the Fut\_CNeutral, Fut\_SSP585, AA\_CNeutral and GHG\_CNeutral simulations.

663

664665



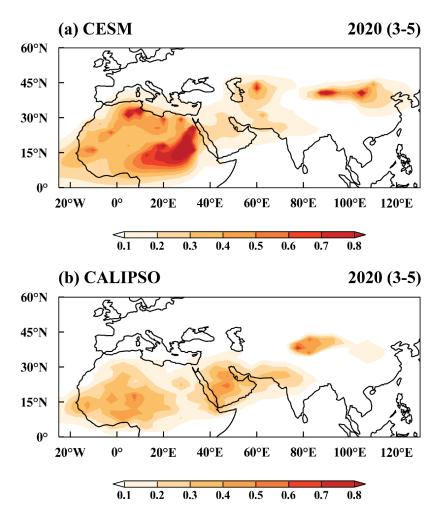


**Figure 2.** Spatial distribution of the average dust optical depth (DOD) from March to May 2020 from (a) the CESM model simulation (Fut\_2020) and (b) the CALIPSO satellite observations.

668

669

670671

672



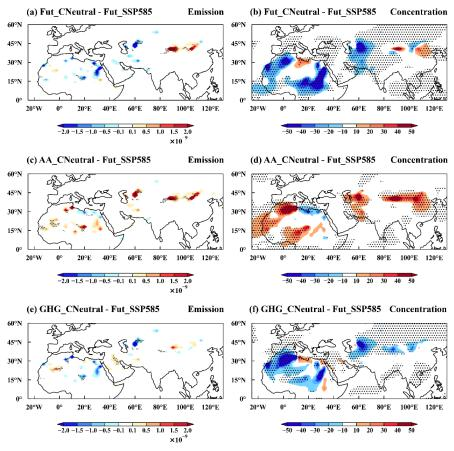


**Figure 3.** Spatial distribution of changes in March–May mean (a, c, e) dust emissions (kg m $^{-2}$  s $^{-1}$ ) and (b, d, f) near-surface dust concentrations (µg m $^{-3}$ ) in 2060 for Fut\_CNeutral (top), AA\_CNeutral (middle), and GHG\_CNeutral (bottom) compared to the Fut\_SSP585 simulation. The stippled areas indicate statistically significant differences at the 90% confidence level based on a two-tailed Student's t test.

674

675

676

677678





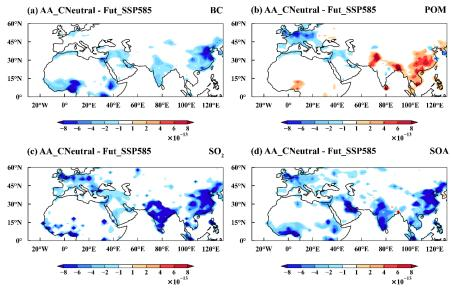


**Figure 4.** Spatial distribution of changes in March–May mean (a) black carbon (BC, kg m<sup>-2</sup> s<sup>-1</sup>), (b) particulate organic matter (POM, kg m<sup>-2</sup> s<sup>-1</sup>), (c) sulfur dioxide (SO<sub>2</sub>, kg m<sup>-2</sup> s<sup>-1</sup>), and (d) precursor gas of secondary organic aerosol (SOAG, Tg m<sup>-2</sup> yr<sup>-1</sup>) in 2060 for AA\_CNeural, compared to the Fut\_SSP585 simulation.



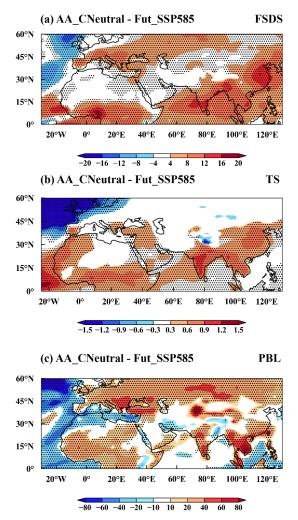


**Figure 5.** Spatial distribution of changes in March–May mean (a) downwelling solar flux at the surface (FSDS, W/m²), (b) surface temperature (TS, K), and (c) planetary boundary layer height (PBL, m), in 2060 for AA\_CNeural, compared to the Fut\_SSP585 simulation. The stippled areas indicate statistically significant differences at the 90% confidence level based on a two-tailed Student's t test.



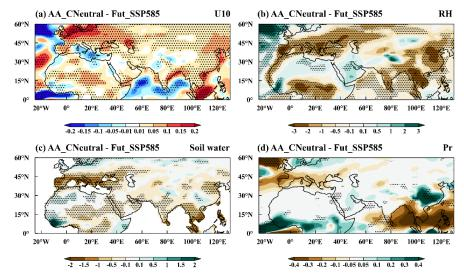


**Figure 6.** Spatial distribution of changes in March–May mean (a) 10-meter wind speed (U10, m s<sup>-1</sup>), (b) relative humidity (RH, %), (c) soil water content (soil water, kg m<sup>-2</sup>), and (d) precipitation rate (pr, mm day<sup>-1</sup>) in 2060 for AA\_CNeural, compared to the Fut\_SSP585 simulation. The stippled areas indicate statistically significant differences at the 90% confidence level based on a two-tailed Student's t test.



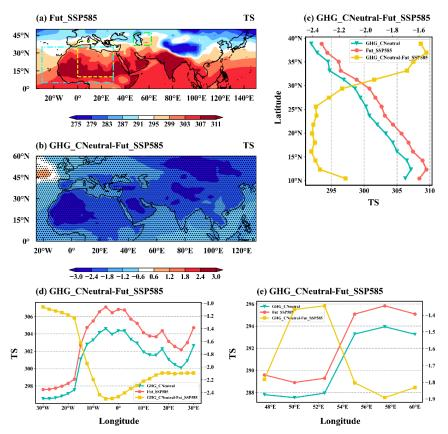


**Figure 7.** Spatial distribution of March–May mean (a) surface temperature (TS, K) in 2060 from Fut\_SSP585 and (b) changes in March-May mean surface temperature (TS, K) in 2060 for GHG\_CNeural, compared to the Fut\_SSP585 simulation. The stippled areas in (a) and (b) indicate statistically significant differences at the 90% confidence level based on a two-tailed Student's t test. (c) Zonal averaged TS (K) over the region (10°–40°N, 0°–30°E, yellow) and (d-e) meridional averaged TS (K) over the regions (5°–35°N, 30°W–30°E, blue; 36.5°–47°N, 47°–62°E, green) marked in (a) from March to May in 2060 for GHG\_CNeutral, Fut\_SSP5-8.5, and the changes between GHG CNeutral and Fut SSP5-8.5.



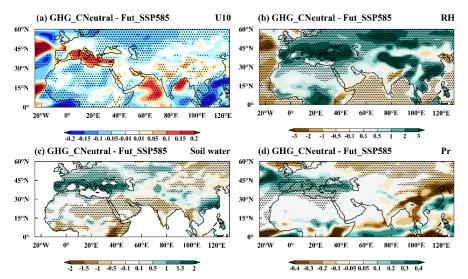


**Figure 8.** Spatial distribution of changes in March–May mean (a) 10-meter wind speed (U10, m s<sup>-1</sup>), (b) relative humidity (RH, %), (c) soil water content (soil water, kg m<sup>-2</sup>), and (d) precipitation rate (pr, mm day<sup>-1</sup>) in 2060 for GHG\_CNeural, compared to the Fut\_SSP585 simulation. The stippled areas indicate statistically significant differences at the 90% confidence level based on a two-tailed Student's t test.

713

714

715716





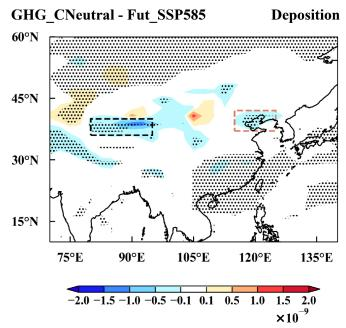


**Figure 9.** Spatial distribution of dust deposition (kg m<sup>-2</sup> s<sup>-1</sup>) changes for the period of March to May in 2060 between GHG\_CNeural and Fut\_SSP585 scenarios. The stippled areas indicate statistically significant differences at the 90% confidence level based on a two-tailed Student's t test. Negative values denote more dust deposition to the surface. The Taklimakan (black box) and North China Plain (brown box) are highlighted.